

Axial-Centric Cross-Plane Attention for 3D Medical Image Classification

Doyoung Park^{1,2}, Jinsoo Kim³, and Lohendran Baskaran^{1,2*}

¹ National Heart Centre Singapore, Singapore

² CVS.AI, National Heart Research Institute of Singapore, Singapore

³ Independent Researcher, Republic of Korea

Abstract. Clinicians commonly interpret three-dimensional (3D) medical images, such as computed tomography (CT) scans, using multiple anatomical planes rather than as a single volumetric representation. In this multi-planar approach, the axial plane typically serves as the primary acquisition and diagnostic reference, while the coronal and sagittal planes provide complementary spatial information to increase diagnostic confidence. However, many existing 3D deep learning methods either process volumetric data holistically or assign equal importance to all planes, failing to reflect the axial-centric clinical interpretation workflow. To address this gap, we propose an axial-centric cross-plane attention architecture for 3D medical image classification that captures the inherent asymmetric dependencies between different anatomical planes. Our architecture incorporates MedDINOv3, a medical vision foundation model pre-trained via self-supervised learning on large-scale axial CT images, as a frozen feature extractor for the axial, coronal, and sagittal planes. RICA blocks and intra-plane transformer encoders capture plane-specific positional and contextual information within each anatomical plane, while axial-centric cross-plane transformer encoders condition axial features on complementary information from auxiliary planes. Experimental results on six datasets from the MedMNIST3D benchmark demonstrate that the proposed architecture consistently outperforms existing 3D and multi-plane models in terms of accuracy and AUC. Ablation studies further confirm the importance of axial-centric query-key-value allocation and directional cross-plane fusion. These results highlight the importance of aligning architectural design with clinical interpretation workflows for robust and data-efficient 3D medical image analysis.

Keywords: Axial-centric multi-planar representation learning · Axial-centric cross-plane attention · 3D medical image classification.

1 Introduction

In clinical practice, three-dimensional (3D) medical images, such as computed tomography (CT) scans, are commonly interpreted using multiple anatomical

* Corresponding author

planes rather than as a single volumetric representation. In multi-planar interpretation, the axial plane serves as the primary acquisition and diagnostic plane, while the coronal and sagittal planes are reconstructed using multiplanar reformation (MPR) to enhance visualization of spatially complex anatomical structures, improving diagnostic accuracy and clinical confidence [1, 2]. Clinicians primarily detect lesions on axial planes and subsequently examine auxiliary planes in a structured manner, reflecting inherently asymmetric dependencies among anatomical planes during clinical decision-making.

Several deep learning (DL) studies have demonstrated that multi-planar approaches outperform single-plane methods by leveraging complementary information across planes [3–6]. Similarly, multiple clinical studies have shown that supplementing the axial plane with coronal and sagittal planes improves diagnostic accuracy and clinician confidence [7–9]. However, many existing multi-planar and 3D DL models treat all planes with equal importance or process the entire 3D volume, resulting in high computational costs and a limited ability to capture asymmetric dependencies between anatomical planes [10, 11]. Consequently, these approaches often fail to reflect how clinicians selectively integrate information across planes, thus limiting robustness and transferability of feature representations in current 3D and multi-planar methods.

Vision foundation models (VFMs) pretrained using self-supervised learning (SSL) on large-scale unlabeled data have demonstrated strong feature extractor capabilities for medical imaging tasks, despite being primarily pretrained on natural images [12, 13]. However, VFMs pretrained on natural images exhibit a distinct feature representation gap compared to those VFMs pretrained on medical images, which limits feature transferability [14]. To address these limitations, Li et al. introduced MedDINOv3 [15], a medical VFM pretrained on 3.87 million axial CT images using DINOv3, demonstrating strong performance in medical image segmentation.

Inspired by clinical interpretation workflows and the robust feature extraction capabilities of VFMs, we propose an axial-centric cross-plane attention architecture for 3D medical image classification. Our approach explicitly models asymmetric inter-plane dependencies between anatomical planes by selectively integrating anatomically relevant information extracted by a medical VFM from auxiliary planes into the axial plane via axial-centric cross-attention, aligning feature representations with clinically meaningful interpretation methods. Experiments on six datasets from the MedMNIST3D benchmark [16] demonstrate that our proposed architecture achieves superior 3D classification performance compared to other architectures evaluated on the same datasets. Our key contributions are as follows:

1. We introduce an axial-centric cross-plane attention architecture that employs a frozen medical VFM as the feature extractor across the axial, coronal, and sagittal planes, enabling data-efficient 3D medical image classification.
2. The axial-centric cross-plane attention is an asymmetric inter-plane cross-attention mechanism that conditions axial feature representations on complementary information from auxiliary planes.

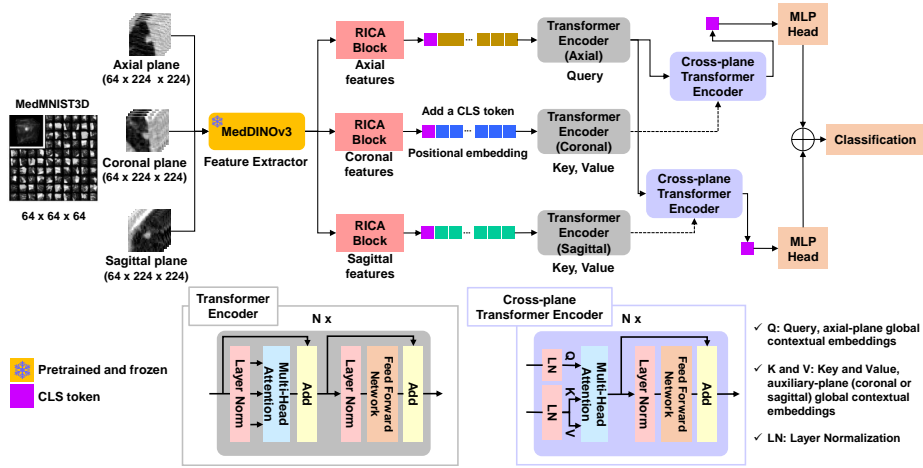


Fig. 1. Overview of the proposed axial-centric cross-plane attention architecture. The architecture comprises a MedDINOv3 backbone for plane-wise feature extraction, RICA blocks for positional context modeling within each stacked feature sequence, transformer encoders for intra-plane contextual self-attention, and axial-centric cross-plane transformer encoders for conditioning axial features on complementary coronal and sagittal information. The fused axial-centric representations are passed to two multilayer perceptron (MLP) heads for final classification.

- Extensive experiments on diverse public 3D medical datasets demonstrate the superior performance of the proposed architecture.

2 Methodology

2.1 Overall Architecture Overview

As illustrated in Fig. 1, the proposed architecture reflects axial-centric clinical reasoning and comprises a MedDINOv3 backbone, RICA blocks, intra-plane transformer encoders, axial-centric cross-plane transformer encoders, and multilayer perceptron (MLP) heads. The MedDINOv3 backbone extracts plane-specific 2D features from volumetric inputs across the axial, coronal, and sagittal planes.

To preserve positional context within each plane, the extracted features are processed by RICA blocks, which serve as CNN-based positional attention modules. Subsequently, transformer encoders are then applied independently to capture long-range contextual dependencies within each plane.

Following intra-plane self-attention, the axial features are independently conditioned on the coronal and sagittal features through axial-centric cross-plane transformer encoders. This asymmetric fusion selectively integrates complementary information from the auxiliary planes while maintaining the axial plane as

the primary reference, consistent with clinical interpretation workflows. Finally, the classification (CLS) tokens from the fused axial-coronal and axial-sagittal representations are processed by MLP heads, and their logits are averaged to produce the final prediction.

2.2 VFM-based Feature Extraction and Positional Context Modeling (RICA)

A medical VFM, MedDINOv3, pretrained on large-scale axial CT images, is employed as a frozen feature extractor across all three anatomical planes as shown in Fig. 1. The inputs consist of single-channel grayscale volumetric data with dimensions $B \times 1 \times D \times H \times W$, where B, D, H, and W represent the batch size, depth, height, and width of the input volume, respectively. Each volume is resized to $B \times 3 \times D \times 224 \times 224$ by duplicating the grayscale channel to match MedDINOv3’s input resolution.

Each 2D slice is independently processed by MedDINOv3 to extract dense feature embeddings [15]. The resulting slice-wise embeddings are then stacked along the depth dimension to form a feature sequence of size $B \times D \times E$, where E denotes the embedding dimension of MedDINOv3. While MedDINOv3 provides robust semantic feature representations at the slice level, highlighting informative positional patterns within the stacked feature sequence is essential for volumetric understanding. RICA blocks [17] are applied to the stacked feature sequences to emphasize positional context by interpreting the $B \times D \times E$ sequences as a pseudo-2D feature map. The RICA block has previously demonstrated effectiveness in highlighting positional information and improving generalization to unseen data in 2D medical image segmentation tasks [17, 18]. These steps are applied independently to the axial, coronal, and sagittal planes, producing plane-specific positional feature representations. Unless otherwise specified, $D = 64$ and $E = 768$ are used in all experiments.

2.3 Intra-plane Transformer Encoder for Contextual Self-Attention

To capture long-range contextual dependencies across non-adjacent slices within each anatomical plane, transformer encoders are applied independently to plane-specific stacked feature sequences. As illustrated in Fig. 1, for each plane, the stacked feature sequence of size $B \times D \times E$ is used directly as the transformer input. Since the features are already embedded by MedDINOv3, no additional linear projection is applied. A learnable CLS token is prepended to aggregate global contextual information across slices. Learnable one-dimensional positional embeddings, including the CLS token, are added to provide spatial order information. The feature sequence from each plane is processed by a plane-specific transformer encoder consisting of $N = 12$ layers and $H = 12$ attention heads, following the standard Vision Transformer (ViT) architecture [19]. This process is applied independently to the axial, coronal, and sagittal feature sequences.

This design preserves plane-specific semantic feature representations while preventing premature fusion across anatomically asymmetric planes, resulting in three plane-specific global contextual embeddings.

2.4 Axial-Centric Cross-Plane Transformer Encoder

In clinical practice, lesion assessment is primarily conducted on the axial plane, with the coronal and sagittal planes subsequently referenced to provide complementary spatial context. Motivated by this asymmetric diagnostic workflow, we introduce an axial-centric cross-plane attention mechanism that conditions axial representations on information from the auxiliary planes while maintaining the axial plane as the primary reference.

Two axial-centric cross-plane transformer encoders are employed for independent fusion of axial features with coronal and sagittal features as shown in Fig. 1. Each encoder processes the plane-specific global contextual embeddings produced by the intra-plane transformer encoders, which include a prepended CLS token. In each case, the axial embedding serves as the query, while the auxiliary-plane embedding (coronal or sagittal) serves as the keys and values, facilitating directional and selective fusion of complementary information rather than symmetric multi-plane aggregation. Each cross-plane transformer encoder is adapted from the intra-plane transformer encoder by replacing self-attention with cross-attention to enable inter-plane feature fusion. The residual connection following the cross-attention is intentionally omitted to reflect the asymmetric setting, where axial queries and auxiliary key-value pairs originate from semantically distinct representations. This omission prevents bias toward the original axial features and facilitates effective cross-plane conditioning. To maintain architectural consistency, the same number of encoder layers ($N = 12$) and attention heads ($H = 12$) as in the intra-plane transformer encoders are used. The CLS token is updated jointly with the slice tokens to aggregate axial-centric global contextual information conditioned on auxiliary planes. Through successive cross-attention layers, the axial query representations are iteratively refined using fixed auxiliary key-value representations, producing fused axial-coronal and axial-sagittal features. This dual cross-attention design facilitates axial-centric yet heterogeneous cross-plane representations, reflecting the stepwise integration of auxiliary-plane information in clinical interpretation workflows.

Finally, the CLS tokens from the fused axial-coronal and axial-sagittal feature sequences are passed to two separate MLP heads. Each head consists of layer normalization followed by two fully connected layers with an embedding dimension E and a \tanh activation function. The \tanh activation function is employed to improve training stability and mitigate overfitting, as MedMNIST3D is a lightweight 3D benchmark dataset. The resulting logits are then averaged to produce the final prediction.

3 Experiments

3.1 Dataset and Experimental Setup

We evaluate the proposed axial-centric cross-plane attention architecture using the MedMNIST+ benchmark, an expanded version of MedMNISTv2 [16, 26]. Within MedMNIST+, MedMNIST3D serves as a standardized benchmark for 3D medical image classification. The datasets cover diverse medical imaging modalities, including CT, magnetic resonance angiography (MRA), and electron microscopy, supporting both binary and multi-class classification tasks. Each dataset is preprocessed into a consistent format and provided with pre-defined training, validation, and test splits to ensure fair comparisons across methods. In this study, we evaluate our architecture on all six MedMNIST3D datasets, each with volumetric dimensions of $64 \times 64 \times 64$. OrganMNIST3D consists of 1,742 abdominal CT volumes with 11 classes (971/161/610 for training/validation/test). FractureMNIST3D comprises 1,370 chest CT volumes with three classes (1,027/103/240). VesselMNIST3D includes 1,908 shapes from brain MRA volumes with two classes (1,335/191/382). SynapseMNIST3D consists of 1,759 electron microscope volumes with two classes (1,230/177/352). NoduleMNIST3D includes 1,633 chest CT volumes with two classes (1,158/165/310). AdrenalMNIST3D contains 1,584 shapes from abdominal CT volumes with two classes (1,188/98/298).

PyTorch container (2.3.0a0+40ec155e58.nv24.03) with Python 3.10.12 was used for all experiments. The experiments were conducted on an NVIDIA DGX-A100 GPU (40 GB) and four CPU cores (64 GB) of an AMD EPYC 7742 processor. The proposed architecture was trained for 100 epochs with a batch size of 4. The Adam optimizer with a cosine annealing warm restart scheduler was employed with an initial learning rate of $1e-12$ and a warm-up period of 5 epochs. The maximum learning rate was set to $1e-4$ for NoduleMNIST3D and $1e-5$ for the remaining datasets. Cross-entropy loss was used for multi-class classification, while binary cross-entropy with logits loss was applied for binary tasks. To improve generalization, six data augmentation methods from the TorchIO library were selectively applied during training: RandomAnisotropy, RandomAffine, RandomFlip, RandomNoise, RandomBlur, and RandomGamma.

3.2 Comparison with Other Methods

We evaluated the proposed architecture on the MedMNIST3D benchmark and compared its performance against six existing methods: a ResNet-18 backbone reported by the official MedMNISTv2 authors [16], BSDA [20], ViViT-M + R-LLM [21], LMTTM-VMI [22], Medformer [23], and CdTransformer + CcCL [24]. Accuracy and area under the ROC curve (AUC), with macro-averaged one-vs-rest AUC for multi-class classification tasks, were used as evaluation metrics. The quantitative results are presented in Table 1.

Overall, our proposed architecture achieved the highest accuracy on five MedMNIST3D datasets and the highest AUC on three MedMNIST3D datasets.

Table 1. Quantitative performance comparison between the proposed axial-centric cross-plane attention architecture and six existing 3D medical image classification models on the MedMNIST3D benchmark. The best results are shown in **bold**. For conciseness, the suffix MNIST is omitted from dataset names. The proposed model uses $N = H = 12$.

Method	Fracture3D		Adrenal3D		Nodule3D		Vessel3D		Organ3D		Synapse3D	
	ACC	AUC										
Official [16]	50.8	71.2	72.1	82.7	84.4	86.3	87.7	87.4	90.7	99.6	74.5	82.0
BSDA [20]	56.9	73.1	83.8	89.2	86.1	89.2	93.2	91.7	88.7	99.4	-	-
ViViT-M + R-LLM [21]	56.3	66.9	83.2	84.9	87.4	88.5	90.6	87.0	-	-	-	-
LMTTM-VMI [22]	56.2	69.1	84.2	84.7	88.3	89.1	93.1	91.7	94.8	99.7	77.7	73.7
Medformer [23]	42.7	53.6	-	-	84.2	87.7	-	-	93.7	99.1	-	-
CdTranformer + CeCL [24]	52.9	72.4	83.6	88.4	90.3	94.3	92.9	95.9	-	-	83.2	87.9
Ours	60.8	71.9	88.6	92.0	89.0	90.2	95.0	93.3	95.7	99.9	86.1	88.0

Table 2. Ablation studies evaluating the effects of model capacity, axial-centric design, and query-key-value (QKV) allocation on the MedMNIST3D benchmark. The best results are shown in **bold**. For conciseness, the suffix MNIST is omitted from dataset names. The small model uses $N = 6$ and $H = 4$, while all other variants employ $N = H = 12$. The proposed full architecture corresponds to the axial-centric cross-plane attention architecture described in the Methodology section. The results highlight the importance of axial-centric QKV allocation and directional cross-plane fusion.

Method	Fracture3D		Adrenal3D		Nodule3D		Vessel3D		Organ3D		Synapse3D	
	ACC	AUC										
Reduced Capacity	56.3	71.7	87.2	91.8	87.4	82.1	94.5	90.9	95.2	99.8	84.1	87.5
Sequential Cross-Plane Fusion	60.4	73.9	88.3	91.6	86.8	84.8	94.0	93.7	94.4	99.8	83.5	84.8
Reversed QKV Allocation	57.1	69.9	84.9	86.1	86.5	87.1	94.2	93.2	89.5	99.3	83.0	84.9
Proposed (Full Architecture)	60.8	71.9	88.6	92.0	89.0	90.2	95.0	93.3	95.7	99.9	86.1	88.0

Notably, it outperformed the second-best method by 3.9% on FractureMNIST3D and by 4.4% on AdrenalMNIST3D in terms of accuracy. On NoduleMNIST3D, our method achieved the second-highest accuracy and AUC, trailing the best-performing method by 1.3% and 4.1%, respectively. These results indicate that the axial-centric cross-plane attention design effectively treats the axial plane as the primary reference while selectively conditioning axial-plane features on complementary information from auxiliary-plane features across diverse modalities, including CT, brain MRA, and electron microscopy.

3.3 Ablation Study

To evaluate the effectiveness of model capacity, axial-centric design, and query-key-value (QKV) allocation, ablation studies were conducted and the results are reported in Table 2. First, reversing the proposed QKV allocation, using auxiliary-plane features as queries and axial features as keys and values, consistently caused substantial performance declines across all datasets. This highlights the importance of employing the axial feature sequence as the query to enable effective axial-centric conditioning. Second, replacing the proposed dual

axial-centric cross-attention modules with a two-stage sequential axial-coronal-sagittal cross-plane fusion resulted in modest performance decreases on most datasets, although there were marginal improvements in AUC for FractureMNIST3D and VesselMNIST3D. This suggests that two independent axial-centric cross-plane fusions are more effective than a sequential multi-planar cross-plane fusion. Finally, reducing model capacity led to subtle performance drops across all datasets, suggesting that architectural design contributes more importantly to performance gains than increased model size.

Overall, these results support the effectiveness of the proposed axial-centric cross-plane attention design and confirm that both the axial-centric QKV allocation and directional cross-plane fusion are important design factors.

4 Conclusion and Future Work

In this work, we propose an axial-centric cross-plane attention architecture for 3D medical image classification, inspired by axial-primary clinical interpretation workflows. By selectively conditioning axial feature representations on complementary coronal and sagittal information, the proposed architecture learns axial-centric yet heterogeneous cross-plane representations aligned with clinical reasoning. Experimental results and ablation studies consistently demonstrate that both axial-centric QKV allocation and directional cross-plane fusion are crucial for performance improvements. These findings highlight the importance of aligning architectural design with clinical interpretation patterns and suggest that axial-centric multi-planar representation learning is an effective and data-efficient method for volumetric medical image classification.

In future work, we plan to evaluate the proposed architecture on higher-resolution institutional cardiac CT and MRI datasets, where multi-planar interpretation is a major diagnostic approach. Additionally, we aim to investigate the impact of alternative large-scale, medical data pretrained models, such as RadImageNet [25], as feature extractors within the proposed architecture.

Acknowledgments. The computational work for this article was fully performed on resources of the National Supercomputing Centre (NSCC), Singapore (www.nsc.sg).

References

1. Ter-Pogossian, M.M.: Basic principles of computed axial tomography. *Semin. Nucl. Med.* **7**(2), 109–127 (1977)
2. Mang, T., et al.: Comparison of axial, coronal, and primary 3D review in MDCT colonography for the detection of small polyps: a phantom study. *Eur. J. Radiol.* **70**(1), 86–93 (2009)
3. Setio, A.A.A., et al.: Pulmonary nodule detection in CT images: false positive reduction using multi-view convolutional networks. *IEEE Trans. Med. Imaging* **35**(5), 1160–1169 (2016)

4. Van Tulder, G., Tong, Y., Marchiori, E.: Multi-view analysis of unregistered medical images using cross-view transformers. In: de Bruijne, M., et al. (eds.) MICCAI 2021, LNCS, vol. 12903, pp. 104–113. Springer, Cham (2021)
5. Black, S., Souvenir, R.: Multi-view classification using hybrid fusion and mutual distillation. In: Proc. IEEE/CVF WACV, pp. 270–280 (2024)
6. Zheng, X., et al.: Xfmamba: Cross-fusion mamba for multi-view medical image classification. In: MICCAI 2025, LNCS, vol. 15960, pp. 672–682. Springer, Cham (2025)
7. McMenamin, D., Pearce, A., Klassen, M.: Visual search in abdominopelvic CT interpretation: accuracy and time efficiency between coronal MPR and axial images. *Acad. Radiol.* **2**(2), 164–168 (2015)
8. Abdelhamid, H.M., et al.: Multiplane reconstruction modifies the diagnostic performance of CT angiography in carotid webs. *Clin. Neurol. Neurosurg.* 244, 108441 (2024)
9. Sandrasegaran, K., et al.: Benefits of routine use of coronal and sagittal reformations in multi-slice CT examination of the abdomen and pelvis. *Clin. Radiol.* **62**(4), 340–347 (2007)
10. Jang, J., Hwang, D.: M3t: three-dimensional medical image classifier using multi-plane and multi-slice transformer. In: Proc. IEEE/CVF CVPR, pp. 20718–20729 (2022)
11. Angkoso, C.V., et al.: Multi-features fusion in multi-plane MRI images for Alzheimer’s disease classification. *Int. J. Intell. Eng. Syst.* **15**(4), 182–197 (2022)
12. Li, Y., Hu, M., Yang, X.: Polyp-sam: Transfer sam for polyp segmentation. In: Proc. SPIE 12927, Medical Imaging 2024: Computer-Aided Diagnosis, 1292735 (2024)
13. Liu, C., et al.: Does DINOv3 Set a New Medical Vision Standard? Benchmarking 2D and 3D Classification, Segmentation, and Registration. arXiv preprint arXiv:2509.06467 (2025)
14. Baharoon, M., et al.: Evaluating general purpose vision foundation models for medical image analysis: An experimental study of dinov2 on radiology benchmarks. arXiv preprint arXiv:2312.02366 (2023)
15. Li, Y., et al.: MedDINOv3: How to adapt vision foundation models for medical image segmentation?. arXiv preprint arXiv:2509.02379 (2025)
16. Yang, J., et al.: MedMNIST v2-a large-scale lightweight benchmark for 2D and 3D biomedical image classification. *Sci. Data* **10**(1), 41 (2023)
17. Park, D., et al.: RICAU-Net: Residual-block Inspired coordinate attention U-Net for segmentation of small and sparse calcium lesions in cardiac CT. In: 2025 IEEE 22nd ISBI, pp. 1–5 (2025)
18. Park, D., et al.: Evaluating the generalizability of an automated coronary artery calcium segmentation and scoring algorithm using multi-vendor dataset. *Sci. Rep.* **15**(1), 21744 (2025)
19. Dosovitskiy, A.: An image is worth 16x16 words: Transformers for image recognition at scale. arXiv preprint arXiv:2010.11929 (2020)
20. Zhu, Y., et al.: BSDA: bayesian random semantic data augmentation for medical image classification. *Sensors* **24**(23), 7511 (2024)
21. Lai, Z., et al.: Residual-based language models are free boosters for biomedical imaging tasks. In: Proc. IEEE/CVF CVPR, pp. 5086–5096 (2024)
22. Wei, H., et al.: LMTTM-VMI: Linked Memory Token Turing Machine for 3D volumetric medical image classification. *Comput. Methods Programs Biomed.* 262, 108640 (2025)
23. Simionescu, C.: Medformer: A Multitask Multimodal Foundational Model for Medical Imaging. *Procedia Comput. Sci.* 270, 446–455 (2025)

24. Zhu, Q., Fu, C., Li, S.: Class-consistent contrastive learning driven cross-dimensional transformer for 3D medical image classification. In: Proc. 33rd IJCAI, pp. 1807–1815 (2024)
25. Mei, X., et al.: RadImageNet: an open radiologic deep learning research dataset for effective transfer learning. *Radiol. Artif. Intell.* **4**(5), e210315 (2022)
26. Yang, J., Shi, R., Ni, B.: Medmnist classification decathlon: A lightweight automl benchmark for medical image analysis. In: 2021 IEEE 18th ISBI, pp. 191–195. IEEE (2021)